Contribution from Lash Miller Chemistry Laboratory and Erindale College, The University of Toronto, Toronto, Ontario, Canada

Cryophotoclustering Techniques for Synthesizing Very Small, Naked Silver Clusters Ag_n of Known Size (Where n = 2–5). The Molecular Metal Cluster–Bulk Metal Particle Interface

GEOFFREY A. OZIN*[1] and HELMUT HUBER

Received June 7, 1977

The technique of photoinduced bulk diffusion and aggregation of Ag atoms, by $^2S_{1/2} \rightarrow {}^2P_{3/2,1/2}$ (315 nm) ultraviolet excitation of high dispersion Ag/Ar $\approx 1/10^5$ to $1/10^3$ matrices at 10–20 K, is found to yield a highly controlled and efficient synthetic pathway to very small silver clusters of known size Ag_n (where n = 2–5). Furthermore, 390-nm photolyses into the A $\rightarrow$ X absorption of argon-entrapped Ag_2 induces what appears to be either photodissociation or a further photoclustering phenomenon in which Ag_3 and Ag_4 molecules are generated. This effect is partly reversible in that $^2S_{1/2} \rightarrow {}^2P_{3/2,1/2}$ photolysis of argon-entrapped atomic silver regenerates Ag_2 and Ag_3. The concepts of localized atomic excitation, electronic to lattice phonon energy transfer, matrix cage softening, short-range bulk diffusion (photomobilization), and photoaggregation are employed to rationalize our experimental observations. These early photoclustering experiments indicate that major improvements over existing surface and bulk diffusion procedures may be realized. In particular, the elimination of troublesome matrix light-scattering effects, which have plagued earlier bulk annealing–aggregation experiments, means that extensive nucleation with $n \geq 2$ can in principle be monitored by optical spectroscopy. Comparisons are also made between silver atom photoclustering experiments and quantitative silver atom–matrix deposition and bulk matrix annealing experiments. Generally, the results indicate that in low dispersion Ag/Ar $\approx 1/10^3$ to $1/10^2$ matrices, extensive silver aggregation can be induced on deposition and after 10–40 K warm-up experiments and can lead to silver clusters with $n \geq 6$ although it is difficult to analyze the deposition process quantitatively for specific values of $n > 3$. Even so, the optical properties of these low-dispersion, quench-condensed films containing small Ag_n clusters with $n \geq 6$ display interesting cluster-size effects with increasing values of n. In essence, the composite optical picture that emerges from the silver cluster system as a function of cluster size is one of a relatively smooth transition from discrete silver atoms, to few-atom clusters containing 2–5 silver atoms having obvious and distinguishable molecular properties, to progressively larger clusters containing roughly 6–15 silver atoms which appear to exhibit *both molecular* and *bulk optical characteristics*, and to still larger silver aggregates which display optical effects most definitely associated with the bulk microcrystalline state, a most significant series of experimental observations if one is to develop a *unified theory* which attempts to naturally bridge the molecular metal cluster–bulk metal microcrystallite interface.

Introduction

Very small transition metal clusters of precisely defined dimensions are of wide ranging interest in heterogeneous particle catalysis[2a–e] and nucleation theory.[2f] Besides their intrinsic value to theoreticians who are concerned with the transition from molecular aggregates of metal atoms to the bulk metal by way of molecular orbital and band theory techniques,[3] "few-atom clusters" are also proving to be experimentally useful for studying localized bonding models of the chemisorbed state.[4] By adopting the metal atom cryosynthetic route, one can in principle generate and spectroscopically probe "pseudo-adsorbate–adsorbent" interactions on "mini transition-metal surfaces" ranging from single- to few-atom sites.[4a,5] In this way some illumination may be brought to bear on the still controversial subject of the chemisorption bond,[2a–e,5,6] particularly, whether it should be treated as a collective property of an infinite, ordered array of metal atoms or rather as a local phenomenon characterized by a limited group of metal atoms in the vicinity of the chemisorption site.[2a–e,5,6]

The present investigation specifically focuses attention on what we believe to be a new and promising metal aggregation phenomenon; its possible applications to supported catalyst synthesis and to studies of the transition from molecular metal clusters to bulk metal microcrystallites as seen through the eye of a matrix optical spectroscopy experiment are most exciting propositions. In brief, we have observed and monitored, for the first time, what appears to be photoinduced bulk diffusion of silver atoms (at low temperatures) to produce silver clusters of known size Ag_n (where n = 2–5). Our motivation for selecting silver atom clustering was governed in part by our standing interest in "chemisorption models" (localized bonding representations) for suspected reaction intermediates (or products) on group 1B heterogeneous oxidation catalysts[4a,7,8a,8b] and a quest for $Ag_n(O_2)$ and $Ag_n(O)$ to simulate $Ag(O_{2chemi})$ and $Ag(O_{chemi})$, respectively.[8c] Additional incentives relate to the scientific and technological importance of the photographic process,[9a,9b] in which silver is clustered in silver bromide, supposedly catalyzed by very small silver clusters in the size range n = 2–4. In this same vein, we note that heterogeneous catalytic silver ion reduction in solution requires a critical-size silver cluster comprised of four atoms of silver.[9c,27] Much theoretical effort has been devoted to modeling the silver latent image process in an attempt to understand the electronic, geometric, and chemical properties of Ag_n and $Ag_n(AgBr)_m$ aggregates as a function of cluster size.[10] Of interest to these discussions are the optical properties (Mie resonances) of colloidal silver particles in the size range 10–1000 Å.[11] Related studies involve the sputtering of silver aggregates up to n = 30 by krypton ion bombardment of silver targets, as monitored by negative ion mass spectroscopy.[12] Finally, one should mention a fascinating x-ray structural determination of a "very small piece of silver metal", to be precise, an octahedral Ag_6 cluster entrapped within the cage of a partially reduced, vacuum-dehydrated, fully Ag^+-exchanged zeolite A.[13] Significantly, recent SCF–Xα–SW model calculations of octahedral clusters M_6 (M = Ni, Cu, Ag) show that they are "large enough" to reproduce trends in energy differences, such as the width of the d bands and the distance from the top of the d bands to the Fermi level, as found in experiment and in bulk energy band calculations.[43]

Experimental Section

The general cryochemical and vacuum furnace arrangement was similar to that described previously.[25] The major difference involved the photolysis equipment which simply comprised an Oriel 200-W xenon lamp and a Jarrel-Ash monochromator band-pass 8 nm. The output of the lamp was focused onto the entrance slit of the monochromator, while the light emerging from the exit slit was allowed

0020-1669/78/1317-0155$01.00/0

to pass through a UV-grade quartz window into the cryostat, where it bathed a 10–12 K sample deposited onto a NaCl optical flat attached to the cold end of a Displex closed-cycle helium refrigeration unit. Ultraviolet–visible monitoring of the photoclusterification process was achieved with a Varian Techtron spectrophotometer in the range 200–900 nm.

Results and Discussion

Photoinduced Bulk Diffusion–Aggregation Experiments. Over the past few years we have succeeded in generating a number of transition-metal homonuclear[14] and heteronuclear[15] diatomic molecules by quantitative metal atom–matrix deposition techniques and have recorded their optical spectra in the 200–900-nm spectral range. Diatomic silver, Ag_2,[14d] actually constituted one of these studies and led to the discovery of the novel silver–silver bonded hexacarbonyl complex $Ag_2(CO)_6$.[16] However, an intrinsic difficulty with metal atom–matrix deposition experiments aimed at generating M_n with $n > 2$ is the design of quantitative high metal–low gas flow conditions. Although it is true that small clusters with $n = 2, 3, 4, 5, 6, \ldots$ may well be present in the matrix support under these conditions, the actual definition of cluster size is often impractical.

A possible way of surmounting these obstacles involves the development of a new technique whereby the less facile and often unpredictable process of bulk diffusion (matrix annealing) of metal atoms is somehow enhanced but in a highly controllable fashion. Although it is well-known that bulk diffusion, by way of controlled annealing procedures, leads to metal aggregation,[14d,17] the method does not appear to lend itself readily to the immobilization and spectroscopic identification of M_n where $n > 2$ but often rather leads to a more catastrophic nucleation phenomenon, in which all cluster absorptions tend to decay, producing a situation invariably characterized by broad, ill-defined absorptions (e.g., plasmon resonances) and highly scattering matrices with baseline complications.[14d,17]

An attractive alternative for inducing a highly controlled and hopefully a predictable form of bulk diffusion and aggregation of metal atoms exploits the idea that "local softening" of the matrix cage at the site of an entrapped metal atom, followed by atom mobilization and clustering, might be arranged photolytically.

Recall that matrix-isolated silver atoms have been extensively studied by ultraviolet–visible[18a-g] and ESR[18h] techniques and the main spectral features have been well-characterized. The ground state is ^2S and gives rise to an absorption spectrum in the ultraviolet, corresponding to the lowest lying $P \leftarrow S$ transition with the ^2P state split by spin–orbit coupling. In the matrix the orbital degeneracy of the $^2P_{3/2}$ level is removed by a crystal-field effect, yielding two sublevels, $P_{3/2\pm1/2}$ and $P_{3/2\pm3/2}$.[18a-g] The matrix spectra in solid Ar generally consist of three intense absorptions (299, 304, 315 nm) and a weaker absorption (322 nm), which can readily be correlated with the spectrum of gas-phase atomic silver by proposing a matrix cage perturbation of the atomic energy levels.

Consider an isolated Ag atom in a 10–12 K argon matrix under high dispersion conditions ($Ag/Ar \approx 1/10^3$) which is excited at the frequency of one of its $4d^{10}5s^1 \rightarrow 4d^{10}5p^1$ atomic resonance transitions (315 nm, Table I).[14d,18a-g] Experimentally, one first observes the gradual decay of all of the Ag atomic resonance absorptions at a rate which appears to be light intensity and time dependent (a typical trace is shown in Figure 1). The known absorptions of argon-entrapped Ag_2 at 387/412, 261/264, and 227 nm[14d,18d,18g,44] can be seen to grow in (Table I, Figure 1) but in a highly controllable manner. In essence, photoclustering of Ag atoms can be initiated and terminated simply by switching the matrix irradiation alternately on and off, respectively. A particularly significant aspect of these Ag/Ar experiments is the observation that with prolonged atomic photolysis new absorptions appear at 245 and 440 nm (Table I, Figure 1) with growth characteristics which are clearly different from those of Ag_2 and which appear to be associated with the second stage (II) of the photoclustering process illustrated in Scheme I.[44] By continuing

Table I. UV-Visible Spectral Data (nm) for the Photoinduced Bulk Diffusion of Ag Atoms in Solid Argon to Yield Ag_n Clusters (Where n = 2–5)

Ag	Ag_2	Ag_3	Ag_4	Ag_5
	227[d]			220[d]
		245		
	261/264		273	
			283	
299[a]				
304				
315[b]				
322				
				333
			347	
			363	
				370
	387/412[c]			
				396
			426	
		440[c]		
			490[c]	
				505[c]

[a] $^2S_{1/2} \rightarrow {}^2P_{3/2\pm3/2}$ atomic Ag transition (see text). [b] $^2S_{1/2} \rightarrow {}^2P_{3/2\pm1/2}$ atomic Ag transition (see text). [c] Assigned as (HOMO-LUMO) transition (see text).[33] [d] Recent studies have indicated that this band could be an impurity[36] and so this assignment should be treated with caution. All other assignments cross-check extremely well for $Ag_{1,2,3,4,5}$ in Kr, Xe, and CH_4 matrices.[36]

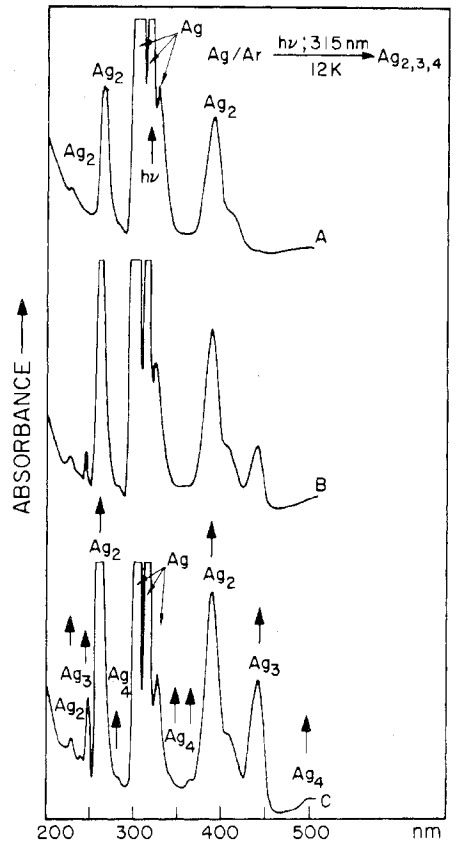

Figure 1. UV–visible spectra of $Ag/Ag_2/Ar$ generated from $Ag/Ar \approx 1/10^3$ depositions: (A) at 10 K; (B) after 15-min, 10–12 K photolysis at 315 nm; (C) after an additional 45-min, 10–12 K photolysis at 315 nm, showing the decay of atomic Ag and the concomitant growth of Ag_2 and Ag_3.

Scheme I

$$Ag + Ag \xrightarrow[315\ nm]{h\nu} Ag_2 \quad (I)$$

$$Ag + Ag_2 \rightarrow Ag_3 \quad (II)$$

$$Ag + Ag_3 \rightarrow Ag_4 \quad (III)$$

$$Ag + Ag_4 \rightarrow Ag_5 \quad (IV)$$

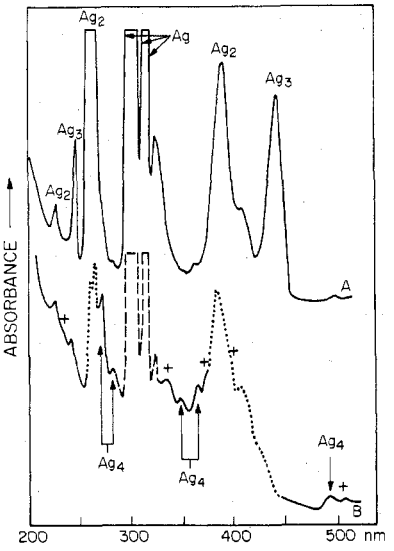

Figure 2. UV–visible spectra of $Ag/Ag_2/Ag_3/Ar$: (A) under conditions similar to those of Figure 1C; (B) after 10-min, 20 K photolysis at 315 nm showing the decay of $Ag_{1,2,3}$ and the concomitant growth of Ag_4 (the cross represents a small amount of Ag_5—see Figure 3 and text).

this photolysis into the 315-nm silver atomic resonance absorption, one observes further Ag atom clustering with the concomitant development of weak new absorptions (with different growth–decay characteristics to Ag, Ag_2, Ag_3) at 273, 283, 347, 363, 426, and 490 nm and 220, 333, 370, 396, and 505 nm. These new absorptions appear to be connected with the third (III)[44] and fourth (IV) stages, respectively, of the silver aggregation sequence to yield Ag_4 and Ag_5 (Table I; Figures 2, 3).

These experiments with silver atoms are reproducible from run to run, showing the presece of at least five resolvable chemical entities which we assign to Ag_n (where $n = 1$–5).[35] In a sense we have devised a kind of "stop-flow matrix kinetics" experiment in which Ag atom diffusion ensues during irradiation and is cryochemically "quenched" when the photolysis terminates. It would therefore appear that photoinduced bulk diffusion processes, at least for silver, are extremely facile, amenable to a high degree of control, and capable of generating small clusters with $n \geq 2$. Certain features of these early experiments are noteworthy. In particular, the elimination of troublesome matrix light-scattering effects, which often plagued earlier bulk annealing–aggregation studies, means that *extensive nucleation* ($n > 2$) can in principle be monitored by optical spectroscopy (and probably ESR, UV, PES, ESCA, MCD, etc.) without the complication of extraneous matrix effects and baseline variations. This discovery represents a major improvement over existing surface and bulk diffusion aggregation procedures. We should note here that by employing mixed-metal, selective-excitation experiments,[19] one can in principle differentiate an energy-transfer process that is localized in the vicinity of the surrounding matrix cage from an extensive lattice-assisted energy-transfer phenomenon (the former appears to be operative in all of the systems that we have so far studied).

We wish to report some other rather fascinating observations which we have witnessed with the Ag/Ar system concerning

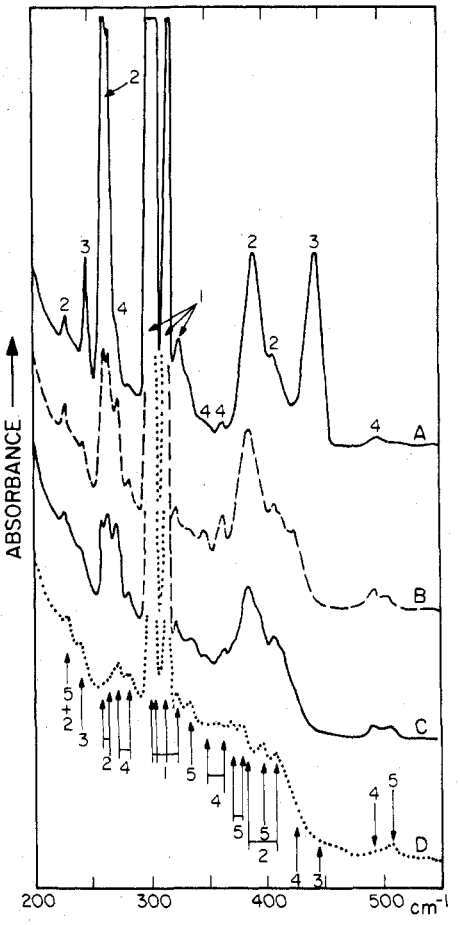

Figure 3. UV–visible spectra of $Ag/Ag_2/Ag_3/Ag_4/Ag_5/Ar$: (A and B) under conditions similar to those of Figure 2A and B; (C) after an additional 10-min, 20 K photolysis at 315 nm; (D) after warm-up to 40 K showing the decay of $Ag_{2,3,4}$ and appearance of Ag_5 and possibly even higher Ag_n clusters.

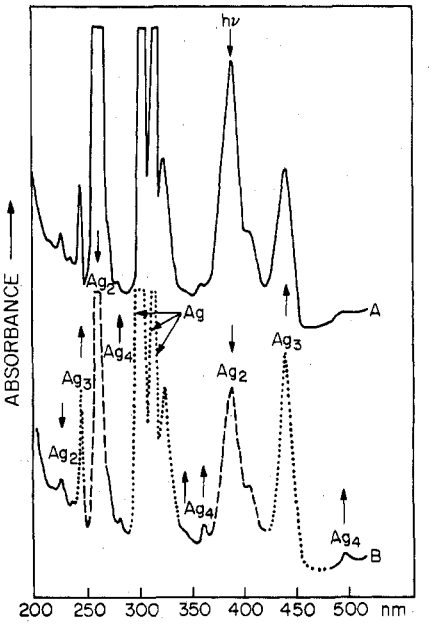

Figure 4. UV–visible spectra of $Ag/Ag_2/Ag_3/Ag_4/Ar$: (A) under conditions similar to those of Figure 1C; (B) after 30-min, 10–12 K photolysis at 390 nm showing the decay of Ag_2 and the concomitant growth of Ag_3 and Ag_4.

what appears to be either a "photodeclustering" phenomenon or "further photoclustering". For example, 390-nm irradiation

into the broad 387/412 nm absorption of Ag_2 in an argon matrix containing mainly Ag, Ag_2, and Ag_3 (Figure 4) causes *growth* of the absorptions associated with Ag_3 and Ag_4 molecules. This effect appears to be partly reversible in that subsequent irradiation into the 315-nm atomic Ag absorption regenerates mainly Ag_2 and Ag_3. The growth and decay characteristics of $Ag_{1,2,3}$ absorptions during Ag and Ag_2 irradiation are not the same, supporting the contention that they are in fact associated with different cluster species.

At this stage of the research we would like to offer some suggestions which might help clarify our intriguing observations with small Ag_n clusters. Let us assume that irradiation into the 315-nm band of atomic Ag excites the $4d^{10}5p^1$ state which subsequently transfers energy to the surrounding matrix cage. (Note that the gas phase to Ar matrix shift of the $^2S \rightarrow {}^2P$ transitions of atomic Ag is 1800–2700 cm^{-1}, which is an order of magnitude greater than kT at room temperature.) Lower energy excited states of atomic silver, into which the $d^{10}p^1$ state could decay, do not exist[20] and it is therefore likely that part or all of the electronic energy of this state (we note here that Gruen and Bates observed no luminescence from B and L SP-200 mercury source irradiation of silver atom–inert gas matrices at 4–13 K[18g]) is channeled into lattice vibrational energy and translational energy of the caged Ag atom; the experimental result is photoinduced bulk diffusion and aggregation of Ag to Ag_n. Although unclear at this early stage, it is likely that Smoluchowski[21] diffusion-controlled kinetic theory can be applied to reactions I–IV for some initial silver atom concentration $[Ag]_0$. Hannay[28] gives the following equation for the rate of decrease of the concentrations of two species A and B which react by diffusion in a solid

$$\frac{-d[A]}{dt} = \frac{-d[B]}{dt} = 4\pi R[D_A + D_B]\left(1 + \frac{R}{[\pi(D_A + D_B)t]^{1/2}}\right)[A][B] \quad (1)$$

where D_A and D_B are the diffusion coefficients of species A and B and R is the radius of a sphere within which A and B are assumed to react instantaneously. If one can show that the only mobile species during Ag atom photolysis is Ag itself,[19] then for typical values of diffusion coefficients in solids and for $R \approx 3$–4 Å, the term $R/(\pi D_{Ag}t)^{1/2}$ will be negligible for values of t (the photolysis time in seconds during which silver atom diffusion–aggregation processes are assumed to take place) in excess of unity. Thus for the sequence of nucleation reactions I–IV eq 1 can be used to derive kinetic expressions of the type

$$\frac{-d[Ag]}{dt} = 4\pi R D_{Ag}[Ag](2[Ag] + [Ag_2] + [Ag_3] + [Ag_4]) \quad (2)$$

$$\frac{d[Ag_2]}{dt} = 4\pi R D_{Ag}[Ag](2[Ag] - [Ag_2]) \quad (3)$$

$$\frac{d[Ag_3]}{dt} = 4\pi R D_{Ag}[Ag]([Ag_2] - [Ag_3]) \quad (4)$$

$$\frac{d[Ag_4]}{dt} = 4\pi R D_{Ag}[Ag]([Ag_3] - [Ag_4]) \quad (5)$$

etc. Remembering that $[Ag]_0$ is a constant, equal to the total silver concentration in the matrix in any form, we can write for our experiment

$$[Ag]_0 = \sum_{n=1}^{n} [nAg_n] \quad (6)$$

Table II. Correlation of Argon-Isolated and Gas-Phase Disilver Ag_2 Absorptions

Ag_2 in Ar (10–12 K)[a,b]		Ag_2 (gas phase)[26] ν, cm^{-1}	Assignment[26]
λ, nm	ν, cm^{-1}		
227[c]	44 053	40 159	E → X
		39 023	D → X
261[d]	38 314	37 626	C → X
264[d]	37 879	35 827	B → X
387/412	25 840/24 272	22 996	A → X

[a] This study. [b] The spectral assignments for Ag_2 are strengthened by comparison with the optical data for the isoelectronic diatomic cation Cd_2^{2+} found in molten $Cd_2(AlCl_4)_2$ (R. A. Potts, R. D. Barnes, and J. D. Corbett, *Inorg. Chem.*, 7, 2558 (1968)):

λ, nm		
Cd_2^{2+}	Ag_2	Band assignment
289	390	$^1\Sigma_g^+ \rightarrow {}^1\Sigma_u^+$
218	260	$^1\Sigma_g^+ \rightarrow {}^1\Pi_u$

where the *blue shifts* on passing from Ag_2 to Cd_2^{2+} are those expected on the basis of the closer approach and greater orbital overlap of the $5s^1$ configuration of Cd^+ compared to Ag. [c] See footnote *d* in Table I. [d] An alternative assignment for these bands is simply a matrix site splitting of the B → X transition.

Considering at this stage the dilute extreme and a gross simplification to a diffusion-controlled dimerization step, one arrives at the expression

$$1/[Ag] - 1/[Ag]_0 = 8\pi R D_{Ag} t$$

for which one would anticipate a roughly linear correlation between the reciprocal of the silver atom absorbance (concentration) and the silver atom photolysis time. This crude description of the photodimerization kinetics essentially mirrors the observed silver atom photodecay in solid argon. The slope, when taken in conjunction with an estimated $[Ag]_0$ value of 7.5×10^{18} atoms cm^{-3} (as determined from our deposition conditions) and R equal to 4×10^{-8} cm, provides an estimate for the "photodiffusion coefficient" $D^{\dagger}_{Ag}$ of atomic silver in solid Ar. This approximate treatment yields a "photodiffusion coefficient" of 6×10^{-19} cm^2 s^{-1} which can be compared with known values of diffusion coefficients of atoms and molecules in low-temperature solids (for example, D_{Cu} in Ar at 35 K, 4×10^{-17} cm^2/s;[14d] D_{CO} in Ar at 30 K, 2×10^{-16} cm^2/s;[29] D_{Sn} in α-N_2 at 34 K, 10^{-18} cm^2/s;[30] D_{Sn} in β-N_2 at 36 K, 10^{-16} cm^2/s[30]). It would therefore appear that photoinduced bulk diffusion of Ag atoms in Ar under 10–12 K reaction conditions is a less facile process than conventional thermally induced–bulk diffusion (annealing) processes occurring in the 30–40 K temperature range. Quantitative photoclustering and thermal clustering experiments are under way for Ag_n (n = 1–5)[36] and other metals in order to further test these ideas as well as the feasibility of establishing cluster size n from absorbance–time curve fitting procedures. In this way we hope to be able to develop a general method for testing simple growth–decay assignments of cluster size of the type employed in the present study.[37]

This simple description of the cryophotoclustering process of Ag atoms to small, well-defined Ag_n clusters explains most of the important experimental observations for Ag atom 315-nm irradiation. On the other hand, 390-nm Ag_2 photolysis could be genuinely photochemical in origin, or a thermally activated diffusion–aggregation process. A possible rationale for these observations takes into account the nature of the cluster electronic transition being excited as well as the metal–metal bond dissociation energy. In the case of Ag_2, the gas-phase[26] and matrix spectra can be correlated reasonably well (Table II) assuming that the lowest energy matrix absorption of Ag_2 (387/412 nm; 25 840/24 272 cm^{-1}; probably experiencing a matrix site symmetry or multiple-site per-

Scheme II

$$Ag_2 \xrightarrow[h\nu]{390\ nm} Ag_2^*$$ (photoexcitation of Ag_2)

$Ag_2^* \rightarrow Ag_2 + h\nu$ (emission from Ag_2)

$Ag_2^* \rightarrow 2Ag^\dagger$ (photodissociation of Ag_2 and photomobilization of Ag)

Scheme III

$$Ag_2 \xrightarrow[h\nu]{390\ nm} Ag_2^*$$ (photoexcitation of Ag_2)

$Ag_2^* \rightarrow Ag_2 + h\nu$ (emission from Ag_2)

$Ag_2^* \rightarrow Ag_2^\dagger + h\nu'$ (emission from Ag_2 and/or photomobilization of Ag_2)

Scheme IV (Assuming Only $Ag^\dagger$ Photomobility)

(a) $Ag^\dagger + Ag \rightarrow Ag_2$
(b) $Ag^\dagger + Ag^\dagger \rightarrow Ag_2$
(c) $Ag^\dagger + Ag_2 \rightarrow Ag_3$
(d) $Ag^\dagger + Ag_3 \rightarrow Ag_4$
(e) $Ag^\dagger + Ag_3 \rightarrow 2Ag_2$
(f) $Ag^\dagger + Ag_4 \rightarrow Ag_5$ etc.

Scheme V (Assuming Only $Ag_2^\dagger$ Photomobility)

(a) $Ag_2^\dagger + Ag \rightarrow Ag_3$
(b) $Ag_2^\dagger + Ag_2 \rightarrow Ag_4$
(c) $Ag_2^\dagger + Ag_2^\dagger \rightarrow Ag_4$
(d) $Ag_2^\dagger + Ag_2^\dagger \rightarrow Ag + Ag_3$
(e) $Ag_2^\dagger + Ag_3 \rightarrow Ag_5$
(f) $Ag_2^\dagger + Ag_3 \rightarrow Ag + Ag_4$ etc.

turbation) corresponds to the gas-phase $A \rightarrow X$ system[26] with $T_e = 22996\ cm^{-1}$. The assignment of the three higher energy absorptions of argon-entrapped Ag_2 (227/261/264 nm; 44053/38314/37879 cm^{-1}) is less certain, although they can be tentatively associated with the gas-phase Ag_2 band systems listed in Table II.[33] Extended Hückel, CNDO,[3c,10] and SCF-Xα-SW[38] molecular orbital calculations for Ag_2 support the assignment of a $^1\Sigma_g^+$ electronic ground state and indicate that the 390-nm transition is probably $\sigma_{5s}^2 \rightarrow \sigma_{5s}^1\sigma_{5s}^{*1}$ in character. Hence 390-nm Ag_2 excitation could populate a state which is Ag–Ag bond weakening and might account for the observed Ag_2 decay. Any excess energy above that required to cause Ag_2 dissociation ($D_e(Ag_2) = 1.63$ eV,[22] $h\nu$(390 nm) = 3.18 eV) could account for the necessary diffusion of the Ag atoms out of the matrix cage to avoid site recombination. With this in mind one can crudely represent the initial photophysical–photochemical events according to Scheme II. One can anticipate from Scheme II lattice diffusion of $Ag^\dagger$ and subsequent reactive encounters with immobilized Ag_n species in the matrix.

On the other hand it is also possible that 390-nm photoexcitation of Ag_2 is not dissociative but rather induces photomobilization of Ag_2 itself according to Scheme III. In this crude description of the photomobilization of Ag_2 we assume $h\nu'$ is zero or less than $h\nu$ as a consequence of nonradiative, electronic to lattice coupling processes. One can envisage from Scheme III lattice migration of $Ag_2^\dagger$ and reactive collisions with immobilized Ag_n species in the matrix. Therefore, depending whether Scheme II or Scheme III (or both) is operative, extremely complex sequences of matrix events could follow 390-nm excitation of Ag_2. Some of these are illustrated in Scheme IV and Scheme V, respectively. Clearly the outcome of these events will be highly dependent on the efficiences of the radiative and nonradiative processes competing for the photoexcited state of Ag_2. Both schemes can readily account for the observed photogeneration of the higher clusters Ag_3 and Ag_4. However, a mechanistic differentiation between Schemes II, IV and III, V must rest heavily on the observation of Ag_2 *decay* yet Ag *constancy*. As silver atom consumption must be assumed in Scheme V(a), one is obliged to counterpropose some form of Ag_n cluster disproportionation process (Scheme V(d)) in order to rationalize the apparent steady-state situation observed for Ag. The observed decay of Ag_2 is, of course, the anticipated outcome of Ag_2 photomobilization followed by further photoaggregation.

Table III. UV-Visible Spectral Data (nm) for Silver Concentration and Bulk Matrix Annealing Experiments for Generating Ag_n Clusters (Where n = 2–7) and Silver Microcrystallites in Solid Argon

Ag[a]	Ag_2[b]	Ag_3[c]	Ag_4[c]	Ag_5[c]	Ag_6[d]	Ag_7[d]	...Ag_n[e]
	227[h]						
		245					
	261/264						
			273				
			283				
299							
304							
315							
322							
				333			
					340		
			347				
							347 → 370[g]
			363				
				370			
	387/412[f]						
				396			
			426				
		440[f]					
			490[f]				
				505[f]			
					520[f]		
						536[f]	

[a–e] Optimum Ag/Ar ratios for generating these Ag_n species are roughly (*a*) $1/10^{4-5}$, (*b*) $1/10^3$, (*c*) 1/300, (*d*) 1/50, and (*e*) 1/20, respectively, plus careful 10–40 K bulk annealing experiments. Note that the "growth-order" frequency assignments of Ag_n (where n = 2–5) based on photoclustering, silver deposition, and bulk matrix annealing techniques are essentially identical. [f] Assigned as (HOMO–LUMO) transition (see text). [g] Assigned to a plasmon resonance of silver microcrystallites whose λ_{max} shifts from 347 to 370 nm on warming Ag/Ar ≈ 1/20 mixtures from 10 to 150 K. [h] See footnote *d* of Table I.

Turning attention to Scheme IV, one can see that a series of nucleation reactions can effectively remove both photomobilized and immobilized silver atoms from their matrix environment. However, to maintain a steady-state concentration of silver atoms, these processes must be approximately counterbalanced by the photogeneration of silver atoms from disilver. Furthermore, the rate of loss of Ag_2 through photodissociation (Scheme II) and nucleation (Scheme IV(c)) reactions must outweigh its rate of production through photoaggregation (Scheme IV(a), IV(b)) reactions. At this point in the Ag_2/Ar cryophotochemistry discussion, one is forced to conclude that Schemes II, IV and III, V appear equally plausible. Further experiments in a variety of matrix supports under different silver concentration conditions are under way to establish the fate of disilver, as well as higher silver cluster photolyses.[36,39]

Metal Atom–Matrix Deposition and Bulk Matrix Annealing–Aggregation Experiments. With these photoclustering effects in mind, let us turn our attention to the optical spectra of small silver clusters obtained by the more conventional metal atom–matrix deposition and bulk matrix annealing–aggregation experiments. In this study we have performed Ag/Ar concentration experiments in the range $1/10^5$ to 1/10 with 10–12 K deposition temperatures. Some typical optical spectra obtained under a variety of deposition and warmup conditions are displayed in Figure 5 and Table III. The general appearance of these optical spectra can be seen to change from a simple, well-defined atomic silver situation (Ag/Ar ≃ $1/10^5$)

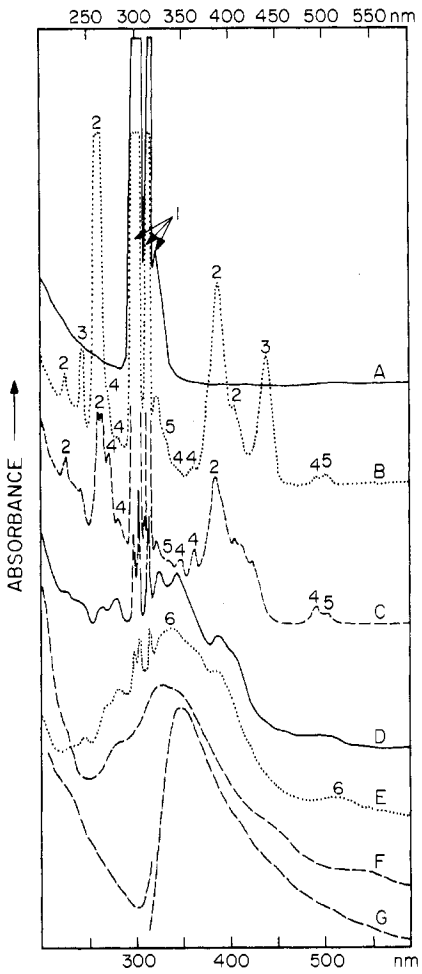

Figure 5. Matrix UV–visible spectra: (A) Ag/Ar ≈ $1/10^5$ deposited at 10 K showing isolated Ag atoms; (B) Ag/Ar ≈ $1/10^3$ deposited at 10 K and photolyzed at 315 nm for 60 min showing clustering into the range $n = 5$; (C) same as (B) but with 10-min, 20 K photolysis at 315 nm showing the loss of most of the Ag_3 absorption with a little more clustering; (D) Ag/Ar ≈ 1/300 deposited at 10 K and warmed to 40 K showing still further clustering to at least $n = 6$; (E) Ag/Ar ≈ 1/50 deposited at 10 K; (F) same as (D) but after warm-up to 40 K showing extensive aggregation, approaching that of (G) Ag/Ar ≈ 1/20 deposited at 10 K in which Ag_n clusters approaching colloidal dimensions (~10 Å) seem to be present as witnessed by the broad, structureless, Mie-type optical resonance centered at roughly 347 nm, *red* shifting to roughly 370 nm on annealing to 100–150 K.

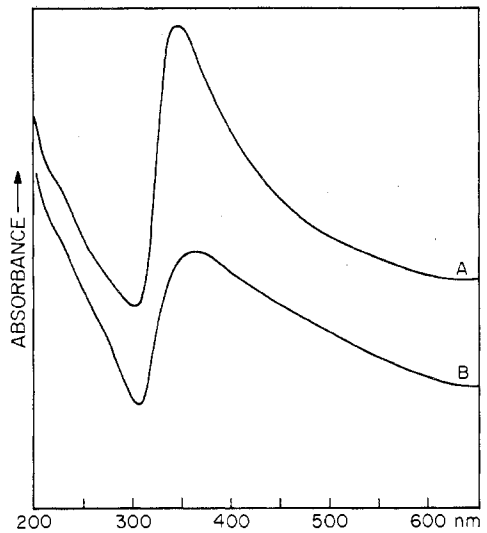

Figure 6. Marix UV–visible spectra of Ag/Ar ≈ 1/20: (A) after deposition at 10 K; (B) after annealing to 40 K showing *red shifting* and *band broadening* behavior typical of a plasmon resonance of a silver aggregate growing in the 10-Å particle size range.[11]

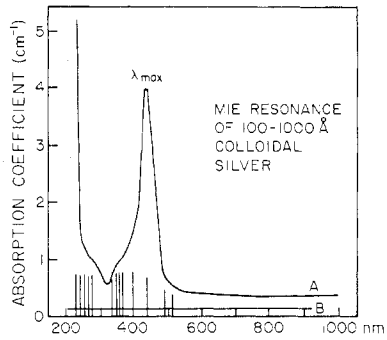

Figure 7. (A) Absorption spectrum of hydrogen-treated $K_\delta Ag_\delta Cl$ crystals (0.06% AgCl; 2-h H_2 treatment at 620 °C) showing the Mie resonance of colloidal silver, whose λ_{max} *red* shifts with increasing silver particle size (taken from ref 11a). (B) Schematic stick diagram representation (arbitrary units) of the absorptions assigned to $Ag_{2,3,4,5}$ of the present study.

in Figure 5A, through varying degrees of spectral complexity (Ag/Ar ≈ $1/10^3$ to $1/10^2$) in Figure 5B–F with band-broadening and band-overlap effects, to a relatively simple picture (Ag/Ar ≈ 1/20) in Figure 5G, where a single, broad, structureless absorption dominates the spectrum at roughly 347 nm. By annealing relatively concentrated Ag/Ar ≈ 1/300 matrices at 40 K (Figure 5D) one can induce silver clustering to at least $n = 6$ as judged by the photoclustering experiments (Figures 2, 3, 5B, 5C). At dispersions lower than 1/300 one moves smoothly toward the kinds of optical resonances that have been well-established for pure silver microcrystallites (deposited onto sapphire at 140 K)[31] as well as large silver aggregates in Ag/Xe ≈ 1/5 mixtures formed at 10 K.[31,32] These types of experiments imply that silver concentration and bulk annealing techniques can be used to cause silver aggregation to the point where the absorbing species can be safely classified as "massive" silver clusters (~10 Å).[11,31]

Some other observations are pertinent here. For example, it would appear that clustering past $n = 2$ by the deposition technique favors $n > 3$ as seen by the appearance of absorptions associated with Ag_4, Ag_5, Ag_6, and higher clusters, although it is not possible to make precise statements about cluster size under these high silver flux–short deposition conditions.[40] At this stage of the clustering process, characteristic absorbances of small Ag_n clusters are still reasonably well-defined (Figure 5C, D, E). However, on progressing to still lower dispersions (Figure 5F, G), band-broadening effects become more pronounced and the optical spectra tend to lose structure and begin to resemble those of plasmon resonances (collective oscillations of conduction electrons) in massive silver aggregates.[11,31] Thus the appearance of broad, featureless absorptions, whose energies tend to shift to longer wavelengths, with concomitant bandwidth enlargements (Figure 6), can readily be rationalized in terms of Maxwell–Garnett[11d] theory of the optical properties of small (with respect to the wavelength of light) spherical metallic islands, modified to take account of changing cluster size.[11e] By reference to the optical spectra of Gomes[11a] for silver aggregates in KCl crystals (Figure 7) one estimates λ_{max}(obsd) 485 nm for spherical particles of 600 Å average diameter (λ_{max} 440 nm). For colloidal silver whose average diameter is very small with respect to the wavelength of the incident light (say 10 Å), λ_{max} is estimated at 400 nm[11a] which is close to the 360–380 nm value found for our 100 K annealed Ag/Ar ≈ 1/20 matrices.

In essence the controlled silver–argon deposition warm-up experiments have permitted the observation of the optical

spectra of "growing" Ag_n clusters, through a size range appropriate for molecular orbital rationalizations of electronic properties into a cluster regime where the optical spectra are best treated in terms of Mie's[11c] general theory for light absorption by silver islands of varying "colloidal" dimensions.

Variation of the Electronic Properties of Silver Clusters with Cluster Size. The Molecular Metal Cluster–Bulk Metal Problem. In this concluding section the fundamental interrelationship between metal cluster size and molecular and bulk particle properties is explored by way of the size dependence of the optical properties of silver aggregates Ag_n in the critical range $2 \leq n \approx 15$. Because of the difficulty of collecting meaningful data in this cluster regime, experimental probes of the crucially important question "how many atoms are needed in a cluster to describe the bulk properties of the metal?" have not hitherto been feasible. The answer to this question will obviously depend upon which properties of the metal one wishes to describe. Some aspects such as bulk cohesive energies, work functions, and effects associated with the Fermi surface may be more critical issues than others, such as bulk electronic and possibly chemisorption properties.

The central theme of our discussion will focus on a critical size criterion of cluster electronic properties, namely, the observation of the optical transformation from discrete, well-resolved molecular cluster absorptions to broad, ill-defined, bulk metal-like plasmon absorptions. In this context the optical properties of silver clusters are especially revealing as they display a rather smooth interconversion between well-defined molecular aggregates (n = 2–5) and bulk metal particles ($n \gtrsim 15$), passing through an intermediate cluster regime ($5 < n \lesssim 15$) which seemingly exhibits both molecular and bulk particle properties. Although a distribution of cluster sizes is inevitable in these types of controlled nucleation experiments, the optical characteristics of the species comprising the lower and upper cluster ranges $1 \leq n \leq 5$ and $n \gtrsim 15$, respectively (see later), are relatively well-defined (at least for Ag_n) and optical correlations (to be described) permit a reasonable view of the middle range $6 \leq n \lesssim 15$.

Before pursuing this idea, let us turn our attention briefly to the theoretical treatments of Ag_n clusters in the size range n = 2–30. Baetzold, Hamilton, and co-workers have used semiempirical molecular orbital methods to evaluate the cohesive energies, density of states, ionization potentials, electron affinities, and minimum energy geometries for Ag_n up to 30 atoms.[3c,10] Of particular note is the prediction of *linear* chains over both two- and three-dimensional structures for "small" Ag_n clusters. Also of interest is the "sawtooth" dependence of the IP's and EA's for linear Ag_n chains in which the even clusters have the largest IP and odd clusters the largest EA values.[3c,10] Incidentally, the normalized mass spectral intensity data for Ag_n^- (n = 2–30) indicate a pronounced odd–even effect of the cluster stability.[12] In this context we wish to point out that the *energy gap* between the HOMO and LUMO as a function of cluster size for linear Ag_n aggregates decreases monotonically, with IP's and EA's converging to a value of roughly 7 eV[3c,10] (close to the work function of bulk silver). These results indicate a *long wavelength* shift in light absorption as particle size increases. We wish to emphasize that this is precisely the trend which we observe experimentally for the lowest energy absorptions ΔE (Figure 9) of small Ag_n clusters as shown below for solid Ar.[23]

	Ag_2	Ag_3	Ag_4	Ag_5	Ag_6	Ag_7
ΔE(obsd), nm	387/412	440	490	505	520	536
ΔE(calcd), nm[a]	404	489	517	581	664	800

[a] Estimated from the data of ref 3c, 10.

If one graphs these ΔE values as a function of $1/n$, a remarkably linear correlation is discovered for n = 1–7 as shown in Figure 8. As the cluster size progresses to values greater than $n \simeq 7$, one observes a gradual broadening of the low-energy optical absorption and a tendency for the band maximum to *red* shift toward a limiting value of roughly 555–570 nm (Figure 9). Interestingly, this low-energy band broadens to disappearance at a cluster value corresponding to $n \approx$ 10–15 as determined from the ΔE vs. $1/n$ extrapolation shown in Figure 8 and for an assumed 3-D cubic close-packed structure (as found in crystalline silver metal itself) calculates close to a 10-Å particle diameter. The significance of these

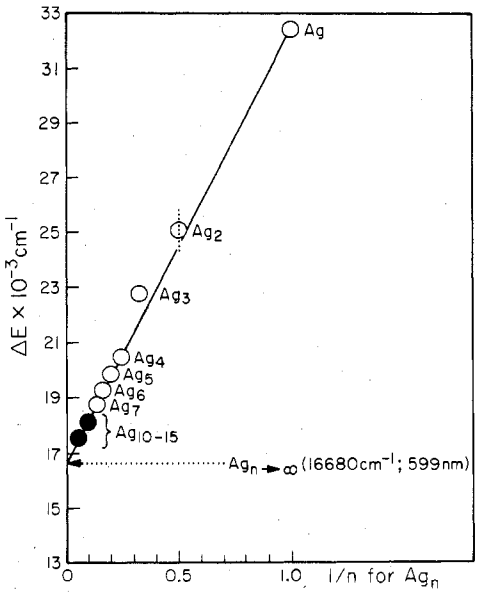

Figure 8. Graphical representation of the energy (cm^{-1}) of the lowest energy absorption of Ag_n (where n = 1–7) as a function of $1/n$ in solid argon. The dotted line on the Ag_2 point represents the energy uncertainty because of the observed 387/412 nm matrix splitting. The Ag_{10} to Ag_{15} points represent the extrapolated cluster sizes corresponding to the lowest energy (HOMO–LUMO) Ag_n absorptions observed in the range 555–570 nm (see text).

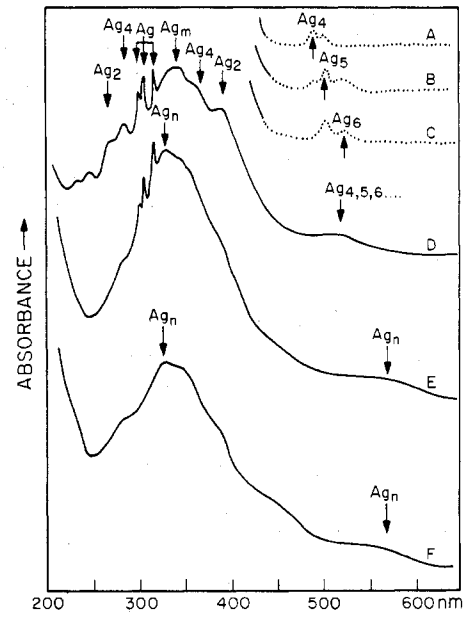

Figure 9. A collection of optical spectra of silver clusters Ag_n (n = 2, 3, 4, 5, 6, ...) isolated in solid Ar at 12 K showing the *red* shifting and broadening behavior of the lowest energy absorption. Note also the growth of broad plasmon resonance-like absorptions in the region of 350–400 nm with superimposed molecular cluster absorptions, the former becoming progressively more pronounced with increasing silver cluster size.

Ag_n observations in terms of cluster model theory[34] is clearly considerable.

The intriguing ΔE vs. $1/n$ linear correlation shown in Figure 8 for Ag_n indirectly suggests a similarity in the nature of the constituent orbitals (at least for $n = 1$–7) associated with the electronic transition responsible for the lowest energy absorption, for example, a silver atom localized s to p excitation.[41] Of special note in these discussions is the *spectral persistence* and monotonic *red* shifting of the lowest energy "molecular cluster absorption" for an estimated $6 \leq n \lesssim 15$ size range (Figures 5, 9) which also appears to display bulk particle properties typified by broad, featureless plasmon absorptions.[43] In this context we wish to draw attention to the recent SCF–Xα–SW calculations for octahedral Ag_6[43] and the x-ray structural determination of a perfectly octahedral Ag_6 cluster entrapped within the cage of zeolite A[13] which can be considered to represent the smallest possible, fully developed, single crystal of silver. Significantly, the onset of the molecular to bulk optical transformations for silver clusters occurs in the vicinity of $n = 6$ and is essentially complete around $n \simeq 10$–15. It is extremely tempting to speculate that these optical effects can be rationalized in terms of a structural interconversion between linear chains for small Ag_n clusters (in line with Baetzold's[3c,10] EH/CNDO–MO predictions, $2 \leq n \leq 5$, typified by discrete, well-resolved molecular absorptions) and a close-packed three dimensional Ag_n array for $n \geq 6$, capable of displaying broad plasmon absorptions arising from collective excitations of all free electrons in the particle. The crucial point that remains to be settled is whether a close-packed cluster in the size range $6 \leq n \lesssim 15$ can exhibit *both* molecular and bulk metal-like optical properties (we note here that for very small particles the plasmon resonance absorbance may be broadened to disappearance[11]) which smoothly move toward the pure bulk particle situation with increasing values of n.

Conclusion

Our discovery of photoinduced bulk diffusion and aggregation of Ag atoms to small, well-defined Ag_n aggregates of known size $n = 2$–5 opens the way to some fascinating experimental and theoretical challenges in the field of metal cluster research. For the case of silver, the technique holds great promise for chemistry and spectroscopy for Ag_n and Ag_nL for n up to at least 5. Moreover, the photoclustering method should provide both complementary and supplementary information to aid our understanding of metal atom–matrix deposition and bulk matrix annealing–clustering experiments. Other early photoclustering successes in our laboratory involving $Cr_{1,2,3}$,[19] $Mo_{1,2,3}$,[19] Cr_nMo_m (where $n, m = 1, 2, 3$),[19] $Cu_{1,2,3,4}$,[42] and $Ni_{1,2,3,4,5,\ldots}$[4a,24] are encouraging indicators of the potential and general utility of the method. Of course, many fundamental questions remain to be answered. These include quantitative studies of the light intensity, metal concentration, matrix support, and matrix temperature dependence of the photoclustering processes. These experiments will form the basis of future research in our laboratory.

Acknowledgment. We are indebted to J. Jortner, W. A. Goddard III, S. Webber, D. Dixon, T. Upton, H. B. Gray, W. Klotzbücher, D. Tyler, and W. Trogler for stimulating discussions of this research. The financial assistance of the National Research Council of Canada, the Atkinson Foundation, the Connaught Fund, Imperial Oil of Canada, Erindale College, and the Lash Miller Chemical Laboratories is also greatly appreciated. This research was completed while G.A.O. was a Sherman Fairchild Distinguished Scholar at the California Institute of Technology. We are indebted to the Division of Chemistry, California Institute of Technology, for their hospitality.

Registry No. Ag, 7440-22-4; Ag_2, 12187-06-3; Ag_3, 12595-26-5; Ag_4, 64475-45-2; Ag_5, 64475-46-3; Ag_6, 64475-47-4; Ag_7, 64475-48-5.

References and Notes

(1) Sherman Fairchild Distinguished Scholar, California Institute of Technology, Pasedena, Calif., 1977.
(2) (a) E. Drauglis and R. I. Jaffee, Ed., "The Physical Basis of Heterogeneous Catalysis", Plenum Press, London and New York, 1975; (b) R. B. Anderson and P. T. Dawson, Ed., "Characterization of Surfaces and Adsorbed Species", Vol. 3, Academic Press, New York, N.Y., 1976; (c) G. A. Somorjai, *Adv. Catal.*, **26**, 2 (1976); (d) R. van Harderveld and F. Hartog, *ibid.*, **22**, 75 (1972); (e) J. H. Sinfelt, *Prog. Solid State Chem.*, **10**, 55 (1975), and references cited therein; (f) F. F. Abraham, "Homogeneous Nucleation Theory", Academic Press, New York, N.Y., 1974.
(3) (a) R. P. Messmer, S. K. Knudsen, K. V. Johnson, J. B. Diamond, and C. Y. Yang, *Phys. Rev. B*, **13**, 1396 (1976); (b) A. Anderson, *J. Am. Chem. Soc.*, **99**, 696 (1977); *J. Chem. Phys.*, **64**, 4046 (1976); **65**, 1729 (1976); (c) R. C. Baetzold, *ibid.*, **55**, 4363 (1971); *J. Catal.*, **29**, 129 (1973); *Adv. Catal.*, **25**, 1 (1975); (d) N. Rösch and T. N. Rhödin, *Faraday Discuss. Chem. Soc.*, **No. 58**, 28 (1974), and references cited therein.
(4) (a) G. A. Ozin, *Catal. Rev.-Sci. Eng.*, in press; *Acc. Chem. Res.*, **10**, 21 (1977); (b) E. P. Kundig, M. Moskovits, and G. A. Ozin, *Angew. Chem., Int. Ed. Engl.*, **14**, 292 (1975); (c) W. A. Goddard III, G. A. Ozin, W. Power, and T. Upton, submitted for publication in *J. Am. Chem. Soc.*; (d) M. Moskovitz and J. Hulse, *Surf. Sci.*, **57**, 125 (1976); **61** 302 (1976); (e) G. A. Ozin, H. Huber, and D. McIntosh, *Inorg. Chem.*, **16**, 3070 (1977); (f) G. A. Ozin and L. Hanlan, *ibid.*, **16**, 2848 (1977), and references cited therein.
(5) (a) R. Ugo, *Catal. Rev.*, **11**, 225 (1975); (b) E. L. Muetterties, *Bull. Soc. Chim. Belg.*, **84**, 959 (1975); **85**, 7 (1976); *Science*, **196**, 839 (1977).
(6) (a) T. B. Grimley, "Molecular Processes on Solid Surfaces", E. Drauglis, R. Gretz, and R. Jaffee, Ed., McGraw-Hill, New York, N.Y., 1969, pp 299–316; (b) B. J. Thorpe, *Surf. Sci.*, **33**, 306 (1972); (c) T. E. Madey, J. T. Yates, Jr., D. R. Sandstron, and R. J. H. Voorhoevre, *Solid State Chem.*, **2**, 1 (1976); (d) L. H. Little, "Infrared Spectra of Adsorbed Species", Academic Press, London, 1966; (e) M. L. Hair, "Infrared Spectroscopy and Surface Chemistry", Marcel Dekker, New York, N.Y., 1967; (f) G. A. Somorjai, *Angew. Chem., Int. Ed. Engl.*, **16**, 92 (1977); (g) J. E. Demuth and D. E. Eastman, *Phys. Rev. Lett.*, **32**, 1123 (1974); (h) G. C. Bond, "Catalysis by Metals", Academic Press, London and New York, N.Y., 1962; (i) H. Conrad, G. Ertl, H. Knozinger, J. Kuppers, and E. E. Latta, *Chem. Phys. Lett.*, **42**, 115 (1976), and references cited therein.
(7) H. Huber, D. McIntosh, and G. A. Ozin, *Inorg. Chem.*, **16**, 975 (1977).
(8) (a) D. McIntosh and G. A. Ozin, *Inorg. Chem.*, **16**, 59 (1977); (b) H. Huber and G. A. Ozin, *ibid.*, **16**, 64 (1977); (c) D. McIntosh and G. A. Ozin, *ibid.*, **15**, 2869 (1976).
(9) (a) J. F. Hamilton, *J. Vac. Sci. Technol.*, **13**, 319 (1976); (b) R. Baetzold, *J. Appl. Phys.*, **47**, 3799 (1976); (c) J. F. Hamilton and P. C. Logel, *Photogr. Sci. Eng.*, **18**, 507 (1974).
(10) (a) R. C. Baetzold, *J. Chem. Phys.*, **55**, 4363 (1971); (b) R. C. Baetzold and E. Mack, *ibid.*, **62**, 1513 (1975).
(11) (a) W. Gomes, *Trans. Faraday Soc.*, **59**, 1648 (1963); (b) E. Rohloff, *Z. Phys.*, **132**, 643 (1952); (c) G. Mie, *Ann. Phys. (Leipzig)*, **25**, 377 (1908); (d) J. C. Maxwell-Garnett, *Philos. Trans. R. Soc. London, Ser. A*, **203**, 385 (1904); **205**, 237 (1906); (e) R. H. Doremus, *J. Appl. Phys.*, **37**, 2775 (1966).
(12) G. Hortig and M. Muller, *Z. Phys.*, **221**, 119 (1969).
(13) Y. Khim and K. Seff, paper presented at the Fourth International Conference on Molecular Sieves, Chicago, Ill., April 18, 1977.
(14) (a) R. Busbey, W. Klotzbücher, and G. A. Ozin, *J. Am. Chem. Soc.*, **98**, 4013 (1976); (b) A. Ford, H. Huber, W. Klotzbücher, E. P. Kundig, M. Moskovits, and G. A. Ozin, *J. Chem. Phys.*, **66**, 524 (1977); (c) E. P. Kundig, M. Moskovits, and G. A. Ozin, *Nature (London)*, **254**, 503 (1975); (d) G. A. Ozin, *Appl. Spectrosc.*, **30**, 573 (1976); (e) W. Klotzbücher and G. A. Ozin, *Inorg. Chem.*, **16**, 984 (1977); (f) L. Hanlan and G. A. Ozin, *ibid.*, **16**, 2848 (1977).
(15) W. Klotzbücher, G. A. Ozin, J. G. Norman, Jr., and H. Kolari, *Inorg. Chem.*, **16**, 2871 (1977).
(16) D. McIntosh and G. A. Ozin, *J. Am. Chem. Soc.*, **98**, 3167 (1976).
(17) See for example: (a) D. W. Green and D. M. Gruen, *J. Chem. Phys.*, **57**, 4462, (1973); **60**, 1797 (1974); (b) W. D. Hewett, Jr., J. H. Newton, and W. Weltner, *J. Phys. Chem.*, **79**, 2640 (1975); (c) J. Hulse and M. Moskovits, *J. Chem. Phys.*, **66**, 3988 (1977); (d) "Cryochemistry", Ed. M. Moskovits and G. A. Ozin, Wiley, New York, N.Y., 1976, and references cited therein.
(18) (a) W. Schulze, D. M. Kolb, and H. Gerischer, *J. Chem. Soc., Faraday Trans.*, **271**, 1763 (1975); (b) F. Forstmann, D. M. Kolb, D. Leutloff, and W. Schulze, *J. Chem. Phys.*, **66**, 2806 (1977), and references cited therein; (c) L. Brewer and B. King, *J. Chem. Phys.*, **53**, 3981 (1970); (d) F. Schock and E. Kay, *ibid.*, **59**, 718 (1973); (e) J. S. Shirk and A. M. Bass, *ibid.*, **49**, 5156 (1968); (f) L. Brewer, B. King, J. L. Wing, B. Meyer, and G. F. Moose, *ibid.*, **49**, 5209 (1968); (g) D. M. Gruen and J. K. Bates, *Inorg. Chem.*, **16** 2450 (1977); (h) P. H. Kasai and D. McLeod, *J. Chem. Phys.*, **55**, 1566 (1971).
(19) (a) W. Klotzbücher and G. A. Ozin, *J. Mol. Catal.*, in press; *J. Am. Chem. Soc.*, in press; both references concerning experimental proof of "photoselective aggregation" through bimetallic cluster techniques.
(20) D. W. H. Carstens, W. Braschear, D. R. Eslinger, and D. M. Gruen, *Appl. Spectrosc.*, **26**, 184 (1972), and references cited therein.

(21) (a) M. Smoluchowski, *Ann. Phys. (Leipzig)*, **48**, 1103 (1915); *Z. Phys. Chem., Stoechiom. Verwandschaftsl.*, **92**, 129 (1917); (b) F. C. Collins and G. E. Kimball, *J. Colloid Sci.*, **4**, 425 (1949).
(22) K. A. Gingerich, *J. Cryst. Growth*, **9**, 31 (1971), and references cited therein.
(23) We note here that this effect is opposite to that recently proposed by Hulse and Moskovits[17c] for Ni_2 and Ni_3.
(24) H. B. Gray, H. Huber, G. A. Ozin, W. Trogler, and D. Tyler, in preparation.
(25) M. Moskovits and G. A. Ozin, *J. Appl. Spectrosc.*, **26**, 481 (1972); E. P. Kundig, M. Moskovits, and G. A. Ozin, *J. Mol. Struct.*, **14**, 137 (1972).
(26) (a) J. Ruamps, *Ann. Phys. (Paris)*, **4**, 1111 (1959); (b) C. Shin-Piaw, W. Loong-Seng, and L. Yoke-Seng, *Nature (London)*, **209**, 1300 (1966).
(27) It is worth noting here that the electronic properties of Ag_4, Ag_4^+, and Ag_4^- have been examined in detail by CNDO and EH techniques.[3c,9,10] Both procedures predict the *linear* form to be the stable neutral cluster, but as the cluster loses electrons the tetrahedral geometry becomes more stable. These effects are in accord with the ESR experiments of R. S. Eachus and M. C. R. Symons, *J. Chem. Soc. A*, 1329 (1970), on the cationic forms of Ag_4 clusters in frozen glasses.
(28) N. B. Hannay, "Solid State Chemistry", Prentice-Hall, Englewood Cliffs, N.J., 1967, p 114.
(29) E. P. Kundig, M. Moskovits, and G. A. Ozin, *Can. J. Chem.*, **50**, 3587 (1972).
(30) A. Bos and A. T. Howe, *J. Chem. Soc., Faraday Trans.*, **70**, 440, 451 (1974).
(31) R. Ryberg and O. Hunderi, *J. Phys. F*, in press; private communication; W. Schulze, H. U. Becker, and H. Abe, Paper 8.5, and T. Welker, Paper 2.9, International Conference on Matrix Isolation, West Berlin, June 21, 1977.
(32) In physical terms, metal particles in the size range 10–1000 Å (called microcrystals) usually display one broad absorption band, which arises from a collective excitation of all free electrons in the particle and can be described in terms of a free-electron gas model.[11] This is to be contrasted with the discrete absorptions of "molecular aggregates" containing a small number of atoms, the mute point being: how many metal atoms constitute "small", within the framework of these discussions? Briefly, collectively displayed free electrons see no repulsive force in the bulk metal and hence zero resonant frequency. However, surface polarization effects in microcrystals produce a field opposite to the electric field of the incident light and cause an absorption maximum (called a plasmon absorption) at finite frequencies.[11] For spherical particles which are small compared to the wavelength of the incident light and which are embedded in a nonabsorbing medium with dielectric constant ϵ_m, the plasmon frequency ω_p is defined by $\epsilon_1(\omega_p) = -2\epsilon_m$ where ϵ_1 is the real part of the dielectric function of the particle.[11] For finite particle density the interaction between the microcrystals must be taken into account by using $\epsilon_1(\omega_p) = -\epsilon_m(2 + Q)/(1 - Q)$ where Q is the volume fraction of small, spherical particles.[11] This effect causes a *long wavelength shift* of the absorption maximum as the size and packing of the particles increases.
(33) We note with great interest that in the emission band system of Ag_2 produced in a silver discharge, Shin-Piaw et al.[26b] found evidence for about 30 bands in the 410–470-nm visible system, degrading to the red, most of which grouped into well-marked sequences which could be well-represented by the usual expression involving the vibration quanta and frequencies of the lower and upper states of the so designated (A–X) system. However, Shin-Piaw et al.[26b] discovered 11 *weak and complicated* bands in a region succeeding the aforementioned band systems at 480.7, 481.1, 486.1, 488.4, 491.5, 491.7, 495.8, 492.2, 499.4, 501.6, and 502.4 nm as well as some complications in the long-wavelength side of the 410–470-nm region which could not be fit into the (A–X) vibrational progression for Ag_2. It was suggested at the time that these bands may be due to polyatomic molecules of silver.[26b] On the basis of our experiments with argon-entrapped Ag_n (where $n = 2$–7) we suggest that the silver discharges of Shin-Piaw et al.[26b] could in fact contain some higher Ag_n clusters. On these grounds further studies of the emission and absorption spectra of gaseous silver clusters Ag_n with $n > 2$ seem justified.
(34) R. P. Messmer in "The Nature of the Surface Chemical Bond", G. Ertl and T. N. Rhodin, Ed., North-Holland Publishing Co., Amsterdam, 1978.
(35) Control photolyses into "window" regions of the spectrum show no effect.
(36) G. A. Ozin, S. Mitchell, and H. Huber, in preparation.
(37) This has now been achieved for $Ag_{1,2,3,4}$.[36]
(38) D. McIntosh and G. A. Ozin, in preparation.
(39) G. A. Ozin and H. Huber, submitted for publication in *J. Am. Chem. Soc.*
(40) Recent, quantitative "silver concentration" experiments in krypton matrices have confirmed our stoichiometric assignments for $Ag_{2,3,4}$ based on quantitative "photoaggregation kinetic experiments".[36]
(41) We are presently attempting to simulate these observations by SCF–Xα–SW transition-state molecular orbital calculations for $Ag_{2,3,4,5,6}$.[38]
(42) S. Mitchell and G. A. Ozin, in preparation.
(43) N. Rösch and D. Menzel, *Chem. Phys.*, **13**, 243 (1976).
(44) We note here that Gruen and Bates[18g] recently reported optical spectra for sputtered silver atoms in Ne and Ar matrices at 5 and 13 K, respectively. By comparison with our photoaggregation/silver concentration/bulk annealing studies, observed bands at 280.5/270.5 and 440.0/244.0/237.5 nm assigned to Ag_2 in Gruen and Bates' optical spectra (Ar matrices) are reassigned to Ag_4 and Ag_3 clusters, respectively.

Contribution from the Department of Chemistry,
The University of Alabama in Huntsville, Huntsville, Alabama 35807

Laser-Induced Chemistry of Diborane

S. SHATAS,[1] D. GREGORY, R. SHATAS, and C. RILEY*[2]

Received May 18, 1977

Diborane was irradiated with the 973-cm^{-1} line of a CW CO_2 laser. The products $B_{10}H_{14}$, B_5H_9, B_5H_{11}, $(BH)_n$, and H_2 resulted in all runs. The number of photons required to produce or transform one molecule of $B_{10}H_{14}$, $B_5H_9 + B_5H_{11}$, H_2, and B_2H_6 was determined at pressures between 64 and 510 Torr with the laser power maintained at 7.85 W. The yields of $B_{10}H_{15}$, $B_5H_9 + B_5H_{11}$, and H_2 produced or B_2H_6 transformed were measured as a function of illumination time at a laser power of 8 W and an initial B_2H_6 pressure of 410 Torr. The number of photons required to produce one molecule of $B_{10}H_{14}$, $B_5H_9 + B_5H_{11}$, and H_2 or transform one molecule of B_2H_6 was determined to be 22 000, 287, 156, and 156 at time zero, respectively. No evidence for a chain process was found, the reaction was not accompanied by light emission, and $B_{20}H_{16}$ was not produced.

Introduction

Although available for some time, the advantages of the high intensity and monochromacity of the chemical laser are just beginning to be realized in synthetic chemistry.[3-5] The ability to enhance desired reaction channels is one of the goals of any synthetic chemist. The multitude of reaction channels opened by thermoequilibrium processes often results in not only many undesirable products but products that may be difficult to separate from those desired. The laser has great potential for simplifying as well as enhancing the yield of desired product during chemical transformation. This intense monochromatic source enables multiple photon absorption which can enhance rate constants orders of magnitude by effectively decreasing the activation energy.

Kompa et al. presented interesting data in 1974 in which CW CO_2 laser experiments on diborane were outlined.[6] Using the R-16 (973 cm^{-1}) line for excitation, they excited the ν-14 wagging mode of B_2H_6.[7] They reported that upon lasing B_2H_6 at various initial B_2H_6 pressures and laser power 11 out of 14 experiments resulted predominantly in the production of icosaborane ($B_{20}H_{16}$). They reported that when $B_{20}H_{16}$ was produced luminescence was also observed and the reaction appeared to be a high quantum yield chain process. However, in 3 out of 14 experiments they reported a slower process not

0020-1669/78/1317-0163$01.00/0